J Therm Anal Calorim (2011) 104:1017–1022
DOI 10.1007/s10973-010-1182-1

# Thermal analysis of *cis*-(dithiocyanato)(1,10-phenanthroline-5,6-dione)(4,4′-dicarboxy-2,2′-bipyridyl)ruthenium(II) photosensitizer

**Kasim Ocakoglu · Fatih M. Emen**

Received: 8 October 2010 / Accepted: 9 November 2010 / Published online: 8 December 2010


**Abstract** Thermal behavior of [*cis*-(dithiocyanato)(1,10-phenanthroline-5,6-dione)(4,4′-dicarboxy-2,2′-bipyridyl) ruthenium(II)], *cis*-[Ru(L1)(L2)$(NCS)_2$] (where the ligands were L1 = 1,10-Phenanthroline-5,6-dione, L2 = 4,4′-dicarboxy-2,2′-bipyridyl) was investigated by DTA/TG/DTG measurements under inert atmosphere in the temperature range of 298–1473 K as well as by XRD analysis of the final product. After making detailed analysis and comparison of thermogravimetrical and MS measurements of ruthenium complex, the decomposition mechanism of that complex was suggested. The values of activation energy and reaction order of the thermal decompositions were calculated by Ozawa Non-isothermal Method for all decomposition stages. The calculated activation energies vary in between 32 and 49 kJ $mol^{-1}$.

**Keywords** Ruthenium complex · Thermal behavior · Dye sensitized solar cell · Polypyridyl complexes · Photosensitizer · Charge transfer sensitizer

## Introduction

Ruthenium metal complexes with polypyridyl ligands receive considerable interest due to their excellent photochemical stability, strong visible absorption, efficient luminescence, and relatively long life metal to ligand charge transition (MLCT) [1–9]. This class of complexes has attracted great interest, not only from science but also from industry side because of the great photovoltaic performance in photovoltaic applications in terms of both conversion yield and long-term stability. It is known in the literature [2] that, such great photovoltaic performance was achieved by using polypyridyl complexes of ruthenium and osmium. Several ruthenium complexes containing anchoring groups such as carboxylic acid, dihydroxy, and phosphonic acid on pyridine ligands have been used as dyes for photovoltaic applications [1–9]. In these complexes, the anchoring groups are responsible for immobilizing the dye on the nanocrystalline $TiO_2$ surface. While their structural properties and applications have been examined extensively, the thermal properties of these compounds received less attention in the literature [10]. The investigation of their thermal stability which limits their usage in applications is very important. Clearly, there remains the need for further research into the thermal properties of these types of ruthenium dyes. Thermal properties of these materials have crucial importance especially for solar cell applications due to the requirement of long-term stability of the sensitizer under the operating conditions. Therefore, it is significant to scrutinize the thermal behaviors of the sensitizer at high temperatures [10].

In this study, we described the thermal behavior of [*cis*-(dithiocyanato)(1,10-phenanthroline-5,6-dione)(4,4′-dicarboxy-2,2′-bipyridyl)ruthenium(II)], *cis*-[Ru(L1)(L2)$(NCS)_2$] (where the ligands were L1 = 1,10-Phenanthroline-5,6-dione and L2 = 4,4′-dicarboxy-2,2′-bipyridyl). The decomposition mechanism was also suggested for ruthenium complex based on the results of thermogravimetrical and MS analysis. The kinetic analysis for all decomposition steps was evaluated by Ozawa Non-isothermal Method.

K. Ocakoglu (✉)
Faculty of Tarsus Technical Education, Mersin University, 33480 Mersin, Turkey
e-mail: kasim.ocakoglu@mersin.edu.tr

F. M. Emen (✉)
Department of Chemistry, Faculty of Arts and Science, Kirklareli University, 39300 Kirklareli, Turkey
e-mail: femen106@gmail.com

## Experimental

All organic solvents were purchased from Fluka and used as received. $[RuCl_2(p\text{-cymene})]_2$, 2,2′-bipyridine-4,4′-dicarboxylic acid, and 1,10-phenanthroline-5,6-dione were purchased from Aldrich. The *cis*-$[Ru(L1)(L2)(NCS)_2]$ complex (Fig. 1) was synthesized according to the literature [3].

The DTA/TG/DTG curves were obtained by a Shimadzu DTG-60H equipped with DTA and TG units. The thermal analysis system was used in the temperature range of 298–1473 K. The samples were placed in Pt crucibles and $\alpha$-$Al_2O_3$ was used as the reference material. Measurements were performed by using a dynamic nitrogen furnace atmosphere with a flow rate of 50 mL $min^{-1}$. Different heating rates were chosen such as 5, 10, and 15 °C/min and the sample mass ranged from 6 to 10 mg. LG/MS-ESI measurement was carried out by an AGILENT 1100 MSD Instrument to identify the gas decomposition products. X-ray powder diffraction analysis of the final residues were made with a Siemens F model diffractometer equipped with an X-ray generator, Phillips, PW-1010 model ranging from 20 to 40 kV and 6 to 50 mA while using a fine focus Cu $K_\alpha$ radiation ($\lambda = 1.5406$ Å).

## Results and discussion

### The thermal stability of *cis*-$[Ru(L_1)(L_2)(NCS)_2]$ complex

The thermal behavior of the ruthenium complex was investigated by using thermal analysis techniques from ambient temperature up to 1473 K under nitrogen atmosphere. The temperature range at which the decomposition occurs, DTA peak positions, and percentage of mass losses of the decomposition reactions were given in Table 1.

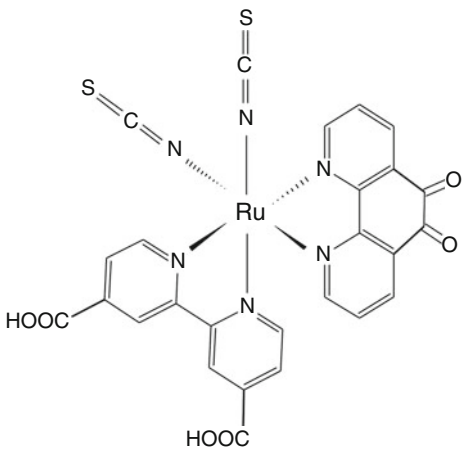


**Fig. 1** The chemical structure of *cis*-$[Ru(L1)(L2)(NCS)_2]$ complex

**Table 1** Thermoanalytical results of decomposition reaction of *cis*-$[Ru(L1)(L2)(NCS)_2]$

| Stage | $DTA_{max}$/K | TG temp. Range/K | Mass loss/% Exper. | Theor. | Evolved moiety |
|---|---|---|---|---|---|
| I | 319 | 298–493 | 11.52 | 11.81 | $-5H_2O$[a] |
| II | 618 | 493–657 | 20.8 | 18.89 | $-2CO$, $-2CO_2$ |
| III | 938 | 657–995 | 21.22 | 20.47 | $-2C_5H_4N$ |
| IV | 1263 | 995–1453 | 34.4 | 35.19 | $-2C_5H_4N$ $-2SCN$ |
| Residue | – | – | 12.64 | 13.25 | Ru |

[a] In the course of thermogravimetric measurements, moisture content can be easily seen due to the hygroscopic properties of the complex

DTA/TG/DTG curves of the *cis*-$[Ru(L_1)(L_2)(NCS)_2]$ complex are presented in Fig 2. It can be seen from the TG curve that the complex exhibits four different decomposition stages. The first decomposition step occurs in the temperature range of 298–493 K. The experimental mass loss was about 11.52% (calc. 11.81%) in this step which corresponds to the elimination of 5 mol of $H_2O$ from coordination sphere of the complex. This result is also compatible with IR measurement that exhibits a broad characteristic peak corresponding to –OH group with hydrogen bonding at 3402 $cm^{-1}$ [3]. The second decomposition was observed in the temperature range of 493–657 K with the experimental mass loss of 20.80% (calc. 18.84%). At this stage, 2 mol of CO and 2 mol of $CO_2$ were eliminated from the molecular structure. Besides, the observed intermediate product was determined as $Ru(SCN)_2(C_{10}H_8N_2)_2$. The experimental mass loss of 21.22% (calc. 20.47%) at the third step corresponding to the elimination of $-2C_5H_4N$ group and the intermediate product of this step was determined as $[Ru(SCN)_2(C_5H_4N)_2]$. At the final decomposition step in the temperature range of 1045–1453 K, the experimental mass loss of 34.40% (calc. 35.19%) corresponds to the elimination of $-2C_5H_4N$ and –2SCN groups was observed. Black-gray colored final product with the mass of 12.64% (calc.13.25) was determined by X-ray powder diffraction techniques as Ru (JCPDS File No: 88-1734). Five endothermic peaks were obtained in DTA profile (see Fig. 2). The minima of these peaks which were due to the formation of intermediate products were found to be at 319, 618, 748, 938, and 1263 K, respectively. In addition to that, DTG peaks are observed at 321, 602, and 947 K at which the mass loss becomes maximum.

According to the data of the TG, MS, and XRD measurements, the suggested decomposition mechanism of the *cis*-$[Ru(L_1)(L_2)(NCS)_2]$ complex is illustrated in Scheme 1. The X-ray powder diffraction pattern and mass spectra are given in Figs. 3 and 4, respectively.

The decomposition kinetic of *cis*-[Ru($L_1$)($L_2$)($NCS)_2$] complex

The kinetic parameters (activation energies, $E_a$; reaction order, $n$; and Arrhenius constant, $A$) of the decomposition process in non-isothermal conditions can be calculated by model-free isoconversional method [11–26]. The non-isothermal kinetic analysis of the thermal decomposition stages was carried out by using data from TG curves obtained with different heating rates (5, 10, and 15 °C/min). Non-isothermal TG measurements of the samples performed at constant heating rates are shown in Fig. 5. TG curves taken at the different heating rates shift to the higher temperatures with an increase in heating rate as expected. If the sample is heated faster, the temperature gradient in the sample gradually increases.

The Ozawa–Flynn–Wall model-free analysis [12–27] was applied to all of the decomposition stages of our compositions in order to calculate the aforementioned kinetic parameters. Concerning to that model, the differential kinetic equation can be written as following:

$$\left(\frac{d\alpha}{dt}\right) = Ae^{-x}f(\alpha) \quad (1)$$

where $A$ is pre-exponential factor and $x = E_a/RT$. By integration of Eq. 1 in non-isothermal conditions, the following equation is obtained:

$$g(\alpha) = \left(\frac{AE}{\beta R}\right)p(x). \quad (2)$$

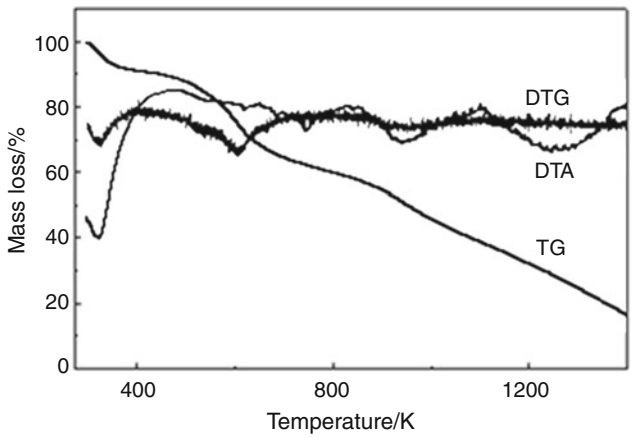


**Fig. 2** DTA/TG/DTG curves of the complex compound

Doyle [14] has suggested that log $p(x)$ can be approximated by the function:

$$\log p(x) = -2.315 - 0.456x. \quad (3)$$

The Eq. 4 can be obtained by combining Eqs. 2 and 3:

$$\log g(\alpha) = \log\left(\frac{AE}{\beta R}\right) - 2.315 - \frac{0.456E}{RT}. \quad (4)$$

The frequency factor is calculated from the equation:

$$\log A = \log g(\alpha)\left[\frac{E}{\beta R}p\left(\frac{E}{RT}\right)\right]. \quad (5)$$

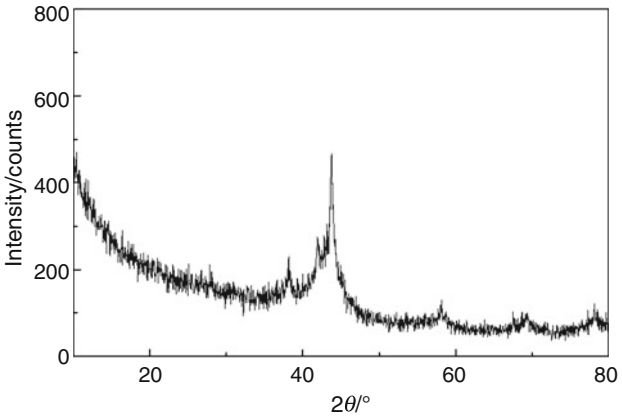


**Fig. 3** X-ray powder diffraction pattern of the decomposition rest product of *cis*-[Ru($L_1$)($L_2$)($NCS)_2$] complex which was identified as metallic ruthenium (JCPDS File No: 88-1734)

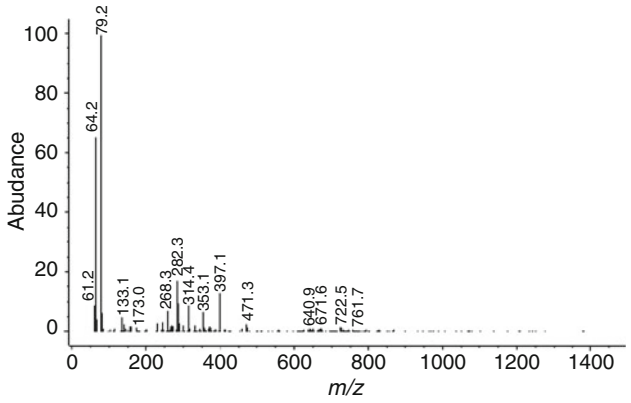


**Fig. 4** Mass spectra of *cis*-[Ru($L_1$)($L_2$)($NCS)_2$] complex

**Scheme 1** The mechanism for the decomposition reaction of the *cis*-[Ru($L_1$)($L_2$)($NCS)_2$] complex

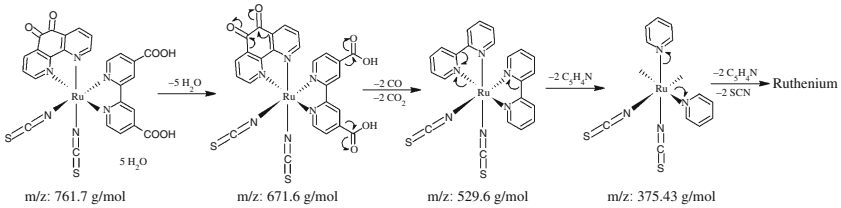

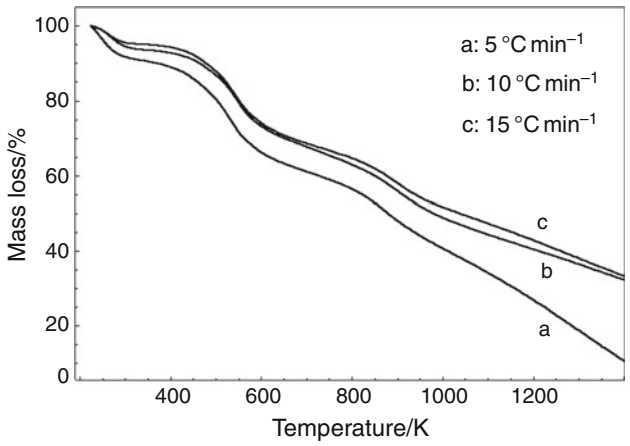


**Fig. 5** The TG curves of the *cis*-[Ru(L$_1$)(L$_2$)(NCS)$_2$] complex at different heating rates (5, 10, 15 °C/min)

For a number of experiments with different heating rates, $\beta$, it can be written for the same extent of reaction $\alpha$:

$$-\log\beta = \frac{0.4567E}{RT} + \text{Constant}. \quad (6)$$

The plot of –log $\beta$ versus 1/$T$ for a given value of $\alpha$ must give the activation energy as suggested by Ozawa [12] and Flynn [27] independently. The average activation energies of the decompositions were calculated as 48.66, 41.74, 32.94, and 40.99 kJ mol$^{-1}$, respectively, for all stages. The calculated kinetic parameters are listed in Table 2. The straight lines obtained from the plot of –log $\beta$ versus the reciprocal of temperature (Eq. 5) at the same degree of conversion are parallel. Ozawa plots of *cis*-[Ru(L$_1$)(L$_2$)(NCS)$_2$] complex are shown in Fig. 6a–d. It can be easily noticed that the activation energies in fourth decomposition stage are similar because of being almost parallel straight lines. However, the activation energies for the other decomposition stages are different from each other because of the unparallel straight lines.

Activation energy versus the degree of conversion for the first, second, third, and fourth decomposition stages of *cis*-[Ru(L1)(L2)(NCS)$_2$] complex based on Ozawa method is given in Fig. 7.

It is shown that the decomposition of the ruthenium polypyridyl complex at the first stage is faster than the others. At the beginning of the first stage, the activation energy is 105.55 kJ mol$^{-1}$ and it decreases down to a value of 27.34 kJ mol$^{-1}$ at the end of this stage. The $E_a$ decreases with a rising of the conversion indicating that the

**Table 2** Kinetic parameters of the decomposition process

| Complex | Step | Activation energy, $E_a$/kJ mol$^{-1}$ | Reaction order, $n$ | Frequency factor, $A$/s$^{-1}$ |
|---|---|---|---|---|
| *Cis*-[Ru(L1)(L2)(NCS)$_2$] | I | 48.66 | 1.00 | $2.775 \times 10^7$ |
| | II | 41.74 | 3.00 | $7.868 \times 10^2$ |
| | III | 32.94 | 0.3 | 3.949 |
| | IV | 40.99 | 0.2 | 1.784 |

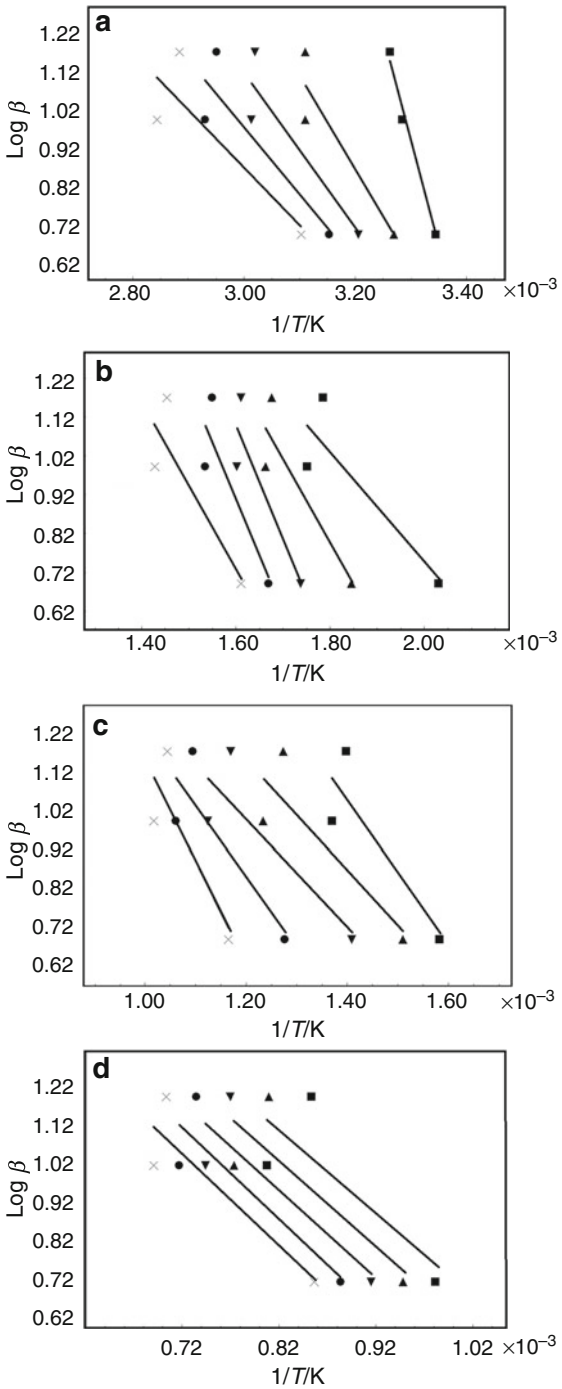


**Fig. 6** Ozawa plots of logarithm of heating rate versus reciprocal temperature (1/$T$) at different conversions for the four decomposition stages of the *cis*-[Ru(L$_1$)(L$_2$)(NCS)$_2$] complex (**a** The first decomposition stage, **b** The second decomposition stage, **c** The third decomposition stage, **d** The fourth decomposition stage)

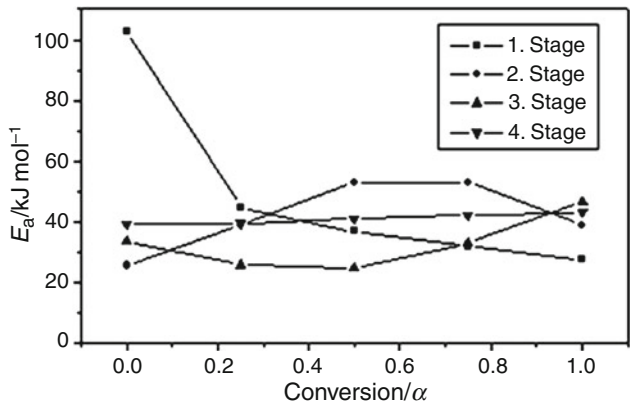


**Fig. 7** Activation energy versus the degree of conversion for the all decomposition stages of *cis*-[Ru($L_1$)($L_2$)($NCS)_2$] complex based on Ozawa method

decomposition reaction contains at least two steps. The activation energy increases from 25.54 to 50.73 kJ mol$^{-1}$ than it drops to 41.74 kJ mol$^{-1}$ at the end of the second decomposition stage. The increase in activation energy with extent of conversion indicates that the second decomposition reaction contains at least two steps. The activation energy of the third stage is 33.54 kJ mol$^{-1}$ at the beginning and it decreases slightly down to 32.94 kJ mol$^{-1}$ with increasing mass loss. The dependence of the activation energy on conversion ($\alpha$) is attributing that the third decomposition reaction contains at least two steps. The activation energy of the fourth stage varies slightly with the degree of conversion and the average activation energy is about 40.99 kJ mol$^{-1}$. Also, the activation energy of the fourth decomposition stage of *cis*-[Ru($L_1$)($L_2$)($NCS)_2$] complex remains relatively constant due to the one dominant kinetic process.

## Conclusions

Thermal behavior of *cis*-[Ru($L_1$)($L_2$)($NCS)_2$] complex, was studied by DTA/TG/DTG analysis under nitrogen atmosphere in the temperature range of 298–1473 K and the final product was identified as metallic ruthenium by XRD analysis. The pyrolytic decomposition mechanism of the complex was suggested depending on the results of the thermal gravimetry and confirmed by MS analysis. The values of activation energy ($E_a$), pre-exponential factor ($A$), and reaction order ($n$) of the thermal decomposition reactions were calculated by Ozawa Non-isothermal Method for all decomposition stages. The values of $E_a$ obtained are in the range of 32–49 kJ mol$^{-1}$ and values of $A$ lie down between 1.784 and 2.775 $\times$ 10$^7$ s$^{-1}$, $n$ varies in between 0.2 and 1.0.

**Acknowledgements** The authors would like to thank The Scientific and Technical Research Council of Turkey (TUBITAK-BAYG) for financial support. The authors thank to Prof. Dr. Nevzat Kulcu, Dr. Göktürk Avsar (from Mersin University, Turkey), and Dr. Selma Erat (ETH-Zurich, Switzerland) for their helpful discussions.

## References

1. Nazeeruddin MK, Humphry-Baker R, Liska P, Grätzel M. Investigation of sensitizer adsorption and the influence of protons on current and voltage of a dye-sensitized nanocrystalline $TiO_2$ solar cell. J Phys Chem B. 2003;107:8981–7.
2. Grätzel M. Thermal analysis of cis-(dithiocyanato)(1,10-phenanthroline-5,6-dione)(4,40-dicarboxy-2,20-bipyridyl)ruthenium (II) photosensitizer. J Photochem Photobiol A Chem. 2004;164:3–14.
3. Ocakoglu K, Zafer C, Cetinkaya B, Icli S. Synthesis, characterization, electrochemical and spectroscopic studies of two new heteroleptic Ru(II) polypyridyl complexes. Dyes Pigment. 2007;75:385–94.
4. Ocakoglu K, Yildirim Y, Lambrecht FY, Ocal J, Icli S. Biological investigation of 131I-labeled new water soluble Ru(II) polypyridyl complex. Appl Radiat Isot. 2008;66:115–21.
5. Ocakoglu K, Yakuphanoglu F, Durrant JR, Icli S. The charge transport and transient absorption properties of a dye-sensitized solar cell. Sol Energy Mater Sol C. 2008;92:1047–53.
6. Xie PH, Hou YJ, Zhang BW, Cao Y, Wu F, Tian WJ, Shen JC. Spectroscopic and electrochemical properties of ruthenium(II) polypyridyl complexes. J Chem Soc Dalton Trans. 1999;23:4217–21.
7. Nazeeruddin MK, Zakeeruddin SM, Humphry-Baker R, Kaden TA, Grätzel M. Determination of pKa values of 4-phosphonato-2,2′:6′,2″-terpyridine and its ruthenium(II)-based photosensitizer by NMR, potentiometric, and spectrophotometric methods. Inorg Chem. 2000;39:4542–7.
8. Rice CR, Ward MD, Nazeeruddin MK, Grätzel M. Catechol as an efficient anchoring group for attachment of ruthenium-polypyridine photosensitizers to solar cells based on nanocrystalline $TiO_2$ films. New J Chem. 2000;24:651–2.
9. Sahin C, Tozlu C, Ocakoglu K, Zafer C, Varlikli C, Icli S. Synthesis of an amphiphilic ruthenium complex with swallow-tail bipyridyl ligand and its application in nc-DSC. Inorg Chim Acta. 2008;361:671–6.
10. Amirnasr M, Nazeeruddin MK, Grätzel M. Thermal stability of cis-dithiocyanato(2,2′-bipyridyl4,4′dicarboxylate) ruthenium(II) photosensitizer in the free form and on nanocrystalline $TiO_2$ films. Thermochim Acta. 2000;348:105–14.
11. Friddman HL. Kinetics of thermal degradation of char-forming plastics from thermogravimetry. Application to a phenolic plastic. J Polym Sci. 1965;6C:183–95.
12. Ozawa T. A new method of analyzing thermogravimetric data. Bull Chem Soc Jpn. 1965;38:1881–6.
13. Uemura K, Kitagawa S, Saito K, Fukui K, Matsumoto K. Thermodynamic aspect of reversible structural conversion induced by guest adsorption/desorption based on infinite $Co(NCS)_2Py_4$ (Py = pyridine) system. J Therm Anal Calorim. 2005;81:529–32.
14. Doyle CD. Estimating isothermal life from thermogravimetric data. J Appl Polym Sci. 1962;6(24):639–42.
15. Alvarez V, Rodriguez E, Vazquez A. Thermal degradation and decomposition of jute/vinylester composites. J Therm Anal Calorim. 2006;85:383–9.
16. Guinesi LS, Ribeiro CA, Crespi MS, Santos AF, Capela MV. Titanium(IV)-EDTA complex. J Therm Anal Calorim. 2006;85:301–7.

17. Vyazovkin S. Computational aspects of kinetic analysis—Part C. The ICTAC kinetics project—the light at the end of the tunnel. Thermochim Acta. 2000;355:155–63.
18. Simon P. Isoconversional methods: fundamentals, meaning and application. J Therm Anal Calorim. 2004;76:123–32.
19. Opfermann JR, Kaisersberger E, Flammersheim HJ. Model-free analysis of thermoanalytical data-advantages and limitations. Thermochim Acta. 2002;391:119–27.
20. Maja T, Sumar R, Dragica MM, Dejan P, Zoran M, Denana M, Katarina KA. Thermal stability and degradation of Co(II), Cd(II), and Zn(II) complexes with *N*-benzyloxycarbonyl glycinato ligand. J Therm Anal Calorim. 2010;102:83–90.
21. Jun Z, Shuangjun C, Jing J, Xuming S, Xiaolin W, Zhongzi X. Non-isothermal melt crystallization kinetics for ethylene–acrylic acid copolymer in diluents via thermally induced phase separation. J Therm Anal Calorim. 2010;101:243–54.
22. Sovizi MR, Anbaz K. Kinetic investigation on thermal decomposition of organophosphorous compounds. J Therm Anal Calorim. 2010;99:593–8.
23. Christos P, Nikolaos K, Stefano V, Maria LK. Lanthanide complexes of 3-methoxy-salicylaldehyde. J Therm Anal Calorim. 2010;99:931–8.
24. Banjong B. Kinetic and thermodynamic studies of $MgHPO_4 \cdot 3H_2O$ by non-isothermal decomposition data. J Therm Anal Calorim. 2009;98:863–71.
25. Stefano V, Romolo DR, Carla F. Kinetic study of decomposition for Co(II)- and Ni(II)-1, 10-phenanthroline complexes intercalated in $\gamma$-zirconium phosphate. J Therm Anal Calorim. 2009;97:805–10.
26. Göktürk A, Hüseyin A, Mustafa KY, Bilgehan G. Synthesis, characterization, and thermal decomposition of fluorinated salicylaldehyde Schiff base derivatives (salen) and their complexes with copper(II). J Therm Anal Calorim. 2010;101:199–203.
27. Flynn JH, Wall LA, Quick A. Direct method for the determination of activation energy from thermogravimetric data. Polym Lett. 1966;4:323–8.